Nearest-neighbor distance distributions and self-ordering in diffusion-controlled reactions. I. $A + A$ simulations

Panos Argyrakis
Department of Physics 313-1, University of Thessaloniki, GR-54006 Thessaloniki, Greece and Department of Chemistry, University of Michigan, Ann Arbor, Michigan 48109-1055

Raoul Kopelman
Department of Chemistry, University of Michigan, Ann Arbor, Michigan 48109-1055
(Received 8 March 1989)

Monte Carlo simulation of transient, diffusion-controlled annihilation ($A + A \rightarrow 0$) and fusion ($A + A \rightarrow A$) reactions have been performed on one- and two-dimensional lattices and on the fractal, critical percolation cluster of a square lattice (applying a breadth-first search algorithm). Fast self-ordering is demonstrated via analyses of the interparticle distributions and the nearest-neighbor distance distributions (NNDD). Good agreement is obtained with the few existing analytical results in one dimension. For the higher dimensions (where there are no analytical results and where the interparticle distances are not uniquely defined), we find the NNDD via a "taxicab" approach. We obtain the kinetically self-ordered particle distributions and relate them to the global rate laws.

I. INTRODUCTION

Diffusion-controlled coagulation (fusion) reactions were first treated by Smoluchowski[1] and have been of interest in astrophysics,[2] materials science,[3] chemistry,[4] biology,[5,6] and engineering.[7] They are often symbolized as $A + A \rightarrow A$, $A + A \rightarrow$ inert, or $A + A \rightarrow$ product. Closely related is the annihilation reaction[3,8-12] $A + A \rightarrow 0$. An important implicit assumption is that any $A + A$ collision results in reaction (with probability unity). Obviously, in the opposite limit (low reaction probability), the overall reaction becomes "reaction limited" rather than diffusion limited. The classical rate laws are always valid for reaction-limited reactions, but important exceptions exist for the diffusion-limited case. While the short-time deviations (from classical theory) have been known since Einstein's work,[8] it is only in the past decade that extreme deviations from the classical picture have been found under long-time and steady-state conditions.[9,10]

While *ex post facto* it is obvious that deviations from the classical rate laws imply that the reacting particle distribution must be partially ordered (rather than randomly distributed),[10] this self-ordering of reactants has only been addressed very recently.[10-12] Actually, the more complicated binary reaction ($A + B$) has been discussed much earlier[13-20] in terms of the reactant self-segregation, which is a special case of self-ordering. The latter ordering can be *macroscopic* and does occur, in principle, in three dimensions (after long times, and with no convection currents). However, it is actually difficult to observe it experimentally. On the other hand, the $A + A$ reactants self-order quickly, but only on a mesoscopic scale and for dimensions below two. Evidence for such self-ordering has been found very recently from simulation,[12,21] from analytical theory,[11] and also from experiments.[12,21]

Quantitative questions of interest are the following. (i) What is the critical dimension for ordering? (ii) What are natural order parameters? (iii) What are the ordered distribution functions? (iv) What is their relation to the global rate laws? (v) Is there a one-to-one relation between them? (vi) Are the distribution functions universal? (vii) Are the theoretically derived asymptotic distribution functions valid at finite times? (viii) What are the effects of steady-state generation? (ix) What is the role of the source term? (x) How good are empirical distribution functions? This work attempts to answer some of these questions.

We find the critical dimension to be two, in accordance with scaling arguments.[14-16,22] The interparticle (gap) distribution in one dimension is skewed-Gaussian (Winger-like[12,21]) for the $A + A \rightarrow A$ reaction, in agreement with Doering and ben-Avraham's analytical form[11] and with earlier simulations.[21] However, for the $A + A \rightarrow 0$ reaction it differs in agreement with the asymptotic arguments of Bramson and Griffeath[23] (and previous simulations[21]), i.e., at long interparticle distances the distribution is fitted by an exponential decay (and at intermediate distances by a skewed exponential). The resulting nonuniversality does not contradict the well-known, universal, global rate laws[10,11,12] (these global rate laws are obtained from a newly derived local rate law).

We also replace the interparticle (gap) distribution functions with nearest-neighbor distance distribution (NNDD) functions, in order to generalize from one to higher dimensions. These NNDD's are also used to define order parameters. The simulations are performed and analyzed for transient fusion ($A + A \rightarrow A$) and annihilation ($A + A \rightarrow 0$) reactions on one- and two-dimensional (square) lattices, as well as on the connected percolation cluster at criticality (on a square lattice). These results for transient reactions are compared to

some results on steady-state reactions.[12,21]

The generalized Hertz NNDD definition,[12,24,25] i.e., the probability density function $P(r)$ for the nearest-neighbor distance r, is adapted to lattices and fractal topologies, using a "taxicab geometry" (see the appendix) that is meaningful for reaction kinetics. (The taxicab geometry is a non-Euclidean geometry, named for its applicability to models of urban geography for the case in which square networks represent the interconnecting streets.) To obtain these modified NNDD functions we use a powerful computer algorithm,[26] breadth-first search (BFS), in connection with the percolation cluster analysis. In contrast, we note that the gap (interparticle) distribution is defined only in one dimension: The distribution of distances between sequential particles.

II. METHOD OF CALCULATIONS

We utilize regular one-dimensional and two-dimensional lattices, and fractal lattices made of percolation clusters exactly at the critical point. The one-dimensional lattices are 10 000 sites long, while the two-dimensional are 200×200 with square planar geometry. The percolation clusters are formed by using binary lattices with the occupational probability p exactly at the critical percolation threshold ($p_c=0.5935$). The largest cluster is isolated using the cluster multiple labeling technique (CMLT).[27] Details of these procedures have been previously reported.[28,29] Typical initial densities are $\rho_0=0.05$ particles/site (see Table I).

TABLE I. Kinetic and distribution data. (N is the number of particles.)

	$A+A\rightarrow0$		$A+A\rightarrow A$	
t	$\langle r\rangle$	N One-dimensional	$\langle r\rangle$	N
0	10.25	500	10.24	500
100	27.13	217.5	20.54	311.8
500	50.83	117.1	33.22	200.1
1000	70.10	85.7	43.70	155.3
2000	97.55	61.8	58.64	116.1
5000	152.54	39.5	89.70	77.0
		One-dimensional gap		
0	19.92	500	19.92	500
100	45.64	217.4	31.92	312.0
500	84.24	117.1	49.64	200.2
1000	114.54	85.7	63.91	155.2
		Two-dimensional		
0	2.88	2000	2.84	2000
100	7.40	332.6	5.74	579.2
500	14.04	91.7	10.31	176.8
1000	18.96	50.6	13.67	99.4
2000	25.84	27.6	18.49	54.7
5000	38.66	12.3	27.63	24.3
		Two-dimensional p_c		
0	5.16	522.3	5.15	520.1
500	23.22	66.03	16.95	121.6
		Three-dimensional		
0		3200		3200
10		1773.1		2281.5
100		385.2		688.2
500		89.1		173.5

The details of the reaction mechanism are as follows: Initially, a certain density of particles is generated randomly on the lattice. No two particles are allowed to occupy the same site, i.e., we impose an excluded volume effect. If a particle happens to fall on top of another particle it is simply not allowed to occupy this site and a new trial is initiated. At this point there is a difference with the Hertz formalism, which is good in the continuum, and therefore has no such effect imposed on it. We thus expect a somewhat longer average interparticle distance than in the Hertz case, and this is exactly what we find. For example, for the one-dimensional lattices, for $\rho_0=0.05$ particles/site, the expected Hertz average interparticle distance is $\langle r\rangle=\int_0^\infty rP(r)dr=1/(2\rho_0)=10$, while our simulation result (Table I) is $\langle r\rangle=10.25$. The average interparticle distance $\langle r\rangle$ is found by first constructing the complete probability distribution function (PDF) $P(r)$ of nearest-neighbor distances. The nearest-neighbor distances are defined via a taxicab geometry.[30] This is fairly straightforward for the case of perfect lattices, as in this method the distances are calculated simply from the difference of the particle x and y coordinates, i.e., $r=|\Delta x|+|\Delta y|$. For a disordered random system, such as a percolation cluster, the situation is somewhat more complicated, as the random voids present in the lattice make the previous method inapplicable. To be kinetically meaningful, the taxicab path is constrained to be only within the cluster. Thus here we use an algorithm[26] called breadth-first search. This algorithm searches for the nearest neighbor of a given particle by first looking only at the immediate neighboring sites. Here, for the square lattice the four nearest neighbors are picked. We label them as visited by this search and place their (x,y) coordinates and distance from the original particle (in this case $r=1$) in a roster, which is kept in memory until the end of the search, i.e., until the nearest neighbor is found. Next, we look for the nearest neighbors of all sites in the previous roster in the same way. We place their coordinates (x,y) and distances r at the end of the roster, one site at a time. Every new site that is encountered is labeled as visited; its distance is simply the distance of the previous (mother) site plus 1. If a site is encountered that does not belong to the largest cluster (nonpermitted site) it is ignored. Thus a traveling wave (breadth) is formed in all directions, but it covers only the region of the largest cluster, and it follows all the random paths of this cluster. Eventually the distance between two particles in whose direct path happens to be a closed site is calculated *around* this site and not *over* it. The process is continued until the first particle is found. This is, by definition, the first neighbor, and its distance is recorded and placed in the PDF. Once the PDF is completed, the average distance $\langle r\rangle$ is found quite simply by averaging over all realizations in our calculation.

The reaction proceeds in the usual way, i.e., all parti-

cles diffuse in the prescribed space by performing random walks. When two particles occupy the same coordinates they react instantaneously, and for the $A+A\rightarrow 0$ reaction both particles are annihilated, while for the $A+A\rightarrow A$ reaction only one of the two particles is eliminated while the second remains on that same site.

III. RESULTS

Figures 1–3 pertain to the one-dimensional reactions. This dimensionality is the only one for which the distance distributions have been calculated theoretically for the interparticle (gap) distances. We note that these distributions have no meaning for $d>1$ (but the NNDD do). Figure 1 shows the NNDD's both for $A+A\rightarrow 0$ and for $A+A\rightarrow A$, for several different times. The x-axis is normalized so that the smallest possible distance ($r=1$) starts at the origin ($x=0$), and all r are also divided by the average value of all distances $\langle r\rangle$. Effectively (within a factor of 2), x is the product $(r)(\rho)$, where ρ is the density. The exponential curve is the NNDD at time $t=0$, i.e., it represents the distribution of a random array of particles. It is in agreement with the Hertz formalism[24,31] (aside from the continuum versus discrete space difference discussed above—see also the Appendix), i.e., it obeys the equation

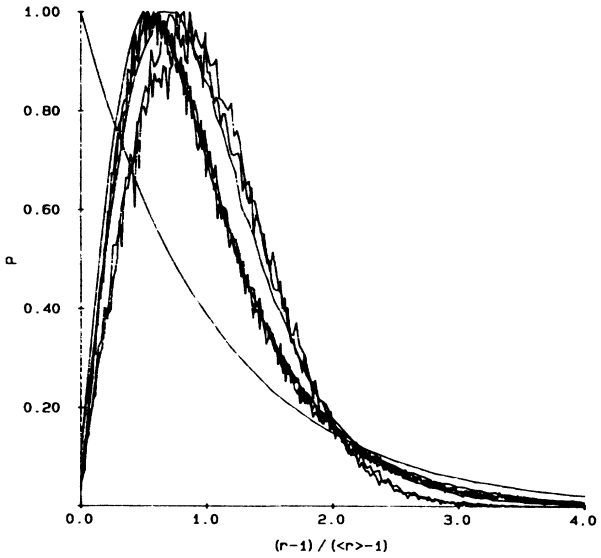

FIG. 1. Normalized distribution of nearest-neighbor distances r for one-dimensional kinetics. The normalization of r is done by calculating the quantity $(r-1)/(\langle r\rangle-1)$, where $\langle r\rangle$ is the average nearest-neighbor distance for all particles at any given time. Lattice size is $L=10\,000$ sites, initial density $\rho_0=0.05$. The exponential single curve is the initial ($t=0$) distribution, the two groups of curves are for the $A+A\rightarrow 0$ reaction (left) and $A+A\rightarrow A$ reaction (right); in each group the distributions are shown for different reaction times: $t=100$, 1000, and 2000 steps. Within each group, due to overlap, it is not meaningful to distinguish the different time curves. All curves are averages of 5000 runs ($A+A\rightarrow 0$) and 1000 runs ($A+A\rightarrow A$).

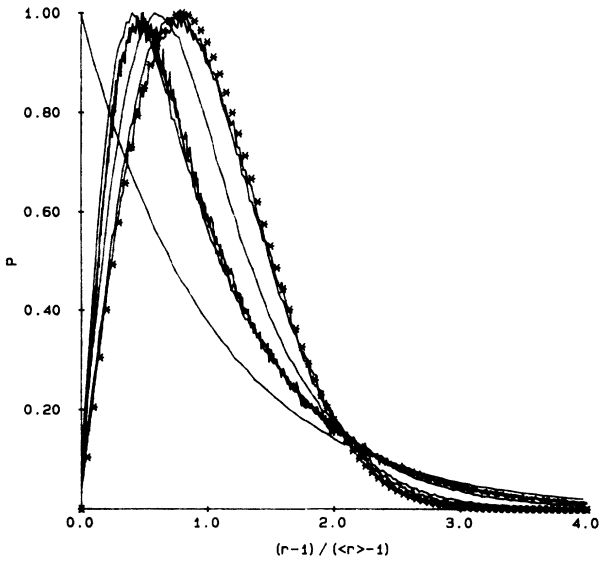

FIG. 2. Similar figure as Fig. 1, but curves show the gap distributions for the same reactions (see text for definitions of gap) 5000 runs each for $t=100$, 500, and 1000. The stars are the solution of the analytical equation of Doering and ben-Avraham, for the $A+A\rightarrow A$ reaction.

$$P(r)=2\rho\exp[-2\rho(r-1)]\ . \tag{1}$$

All probabilities are normalized to 1.00. We notice that for times up to 2000 steps all curves almost coincide for each case. Most of the differences between $t=1000$ and 2000 are not significant. This means that the kinetic limit is reached fairly fast. We extended the calculation up to $t=5000$ steps, with results similar to these shown here; these are not included in the figure as, due to the low density, they contain substantial noise.

Figure 2 gives the interparticle (gap) distributions for the same systems as in Fig. 1. Here we have a recent continuum formalism[11] with which to compare results

$$P(r)=(\pi/2)z\exp[-(\pi/2)z^2/2]\ \text{ as } t\rightarrow\infty\ , \tag{2}$$

where $z=\rho(t)r$, and $\rho(t)$ is the time-dependent particle concentration. This result is also shown in Fig. 2, and we see that it is in good agreement with our calculations. We note that Eq. (2) is very similar (an accident?) to the Hertz NNDD for *random* particle distributions in *two* dimensions (see the Appendix):

$$P(r)=(\pi/2)\langle r\rangle^{-1}r\exp[-(\pi/4)(r/\langle r\rangle)^2]\ . \tag{3}$$

Figure 3 shows a plot versus $[(r-1)/(\langle r\rangle-1)]^x$ of the function P', where P' is defined as

$$P'=\ln P-\ln(r/\langle r\rangle)+\ln\langle r\rangle\ . \tag{4}$$

For the $A+A\rightarrow A$ reaction we get a straight line, in accordance with Eq. (2), with a slope of 0.788. The predicted value from Eq. (2) is $\pi/4(=0.785)$. The two-dimensional random NNDD (Hertzian, but on a square lattice with taxicab geometry— see the Appendix) also

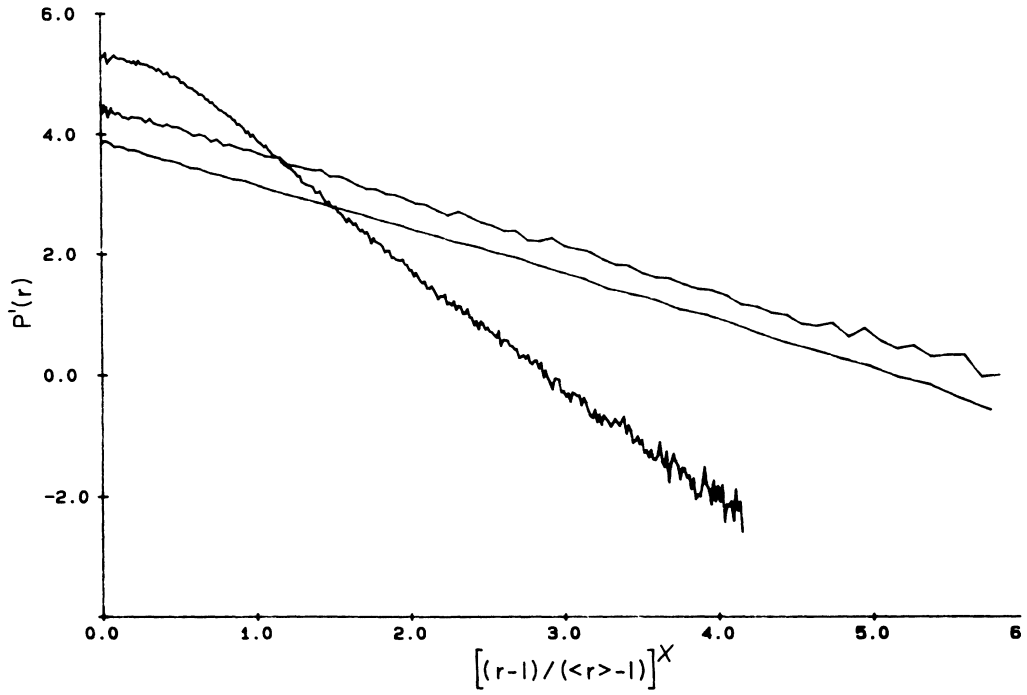

FIG. 3. Plot of the distribution function $P'(r)$ vs $[(r-1)/(\langle r\rangle-1)]^x$. We define $P'(r)=\ln P-\ln(r/\langle r\rangle)+\ln(\langle r\rangle)$. x is an exponent whose value we use as a parameter. On the top two lines $x=1$, while on the bottom $x=2$. Shown are (top to bottom, right-hand side): one-dimensional $A+A\rightarrow A$ ($t=1000$ steps), two-dimensional random ($t=0$), one-dimensional $A+A\rightarrow 0$.

shows the same functional behavior, as expected from Eq. (3), as well as the same slope (within the simulation error). On the other hand, the one-dimensional $A+A\rightarrow 0$ reaction has a very different functional form. For large values of $r(r\gg\langle r\rangle)$ the distribution appears to be exponential (Poissonian) as expected asymptotically by Bramson and Griffeath[23] and Bramson and Lebowitz.[32] However, the attempted fit with the empirical function

$$P(r)\sim\rho r\exp(-\alpha\rho r) \tag{5}$$

is not very good (Fig. 3).

Figure 4 shows the NNDD's for the two-dimensional reactions. We notice that the initially random ($t=0$) case, and the two kinetic cases ($A+A\rightarrow 0$ and $A+A\rightarrow A$) are all described by similarly looking curves. The random function is in agreement with the Hertz function (see above).

Figure 5 shows the kinetics on a two-dimensional fractal lattice. This is a percolation cluster exactly at the critical point p_c. The NNDD is derived using the BFS technique, as described in Sec. II. We observe a behavior qualitatively similar to that of the square lattice. However, the kinetic distributions seem to deviate more from the random distribution.

Figure 6 emphasizes the initial (smallest distance) parts of the various NNDD's. These can all be approximated asymptotically (for $r\rightarrow 0$) as simple algebraic (power) functions $P(r)\sim r^x$, except for the purely exponential one-dimensional Hertz function ($t=0$). The kinetic

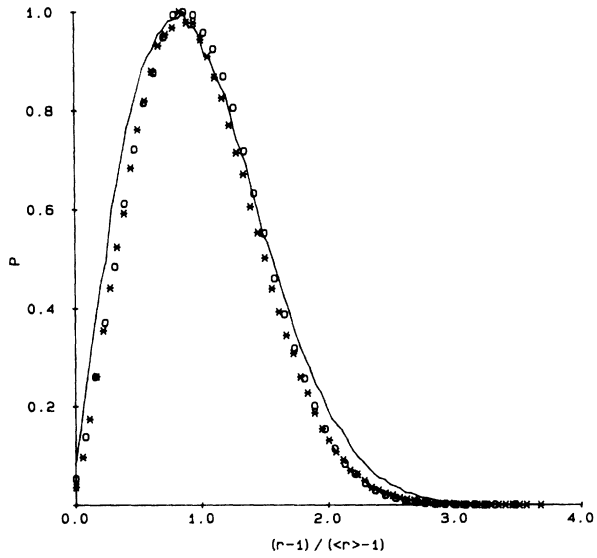

FIG. 4. Normalized distribution of nearest-neighbor distances r for two-dimensional kinetics. The normalization is done similarly to the one-dimensional data. Shown are the $A+A\rightarrow 0$ (1000 runs, stars), and the $A+A\rightarrow A$ (5000 runs, circles) after $t=1000$ steps. The lattices used were 200×200 in size in the initial density $\rho_0=0.05$. The random curve shown (solid) is calculated from a low density of $\rho=0.000\,625$, which is the particle density at $t=1000$ (10 000 runs).

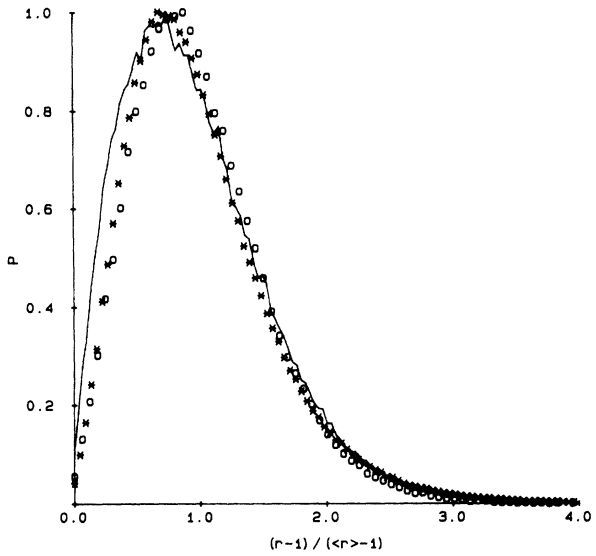

FIG. 5. Distribution $P(r)$ for fractal two-dimensional lattice kinetics. The data here is for $\rho_0=0.05$ from calculations similar to that in Fig. 4, but the reaction here is limited to the largest percolating cluster at the critical point. 10000 runs for the $A+A\rightarrow 0$ (stars) kinetic data ($t=500$) and 1000 runs for the $A+A\rightarrow A$ (circles, $t=500$). The random curve (solid) is for a low density (7000 runs).

($t=1000$) functions in one dimension are consistent with $x=1$, in agreement with the analytical solution[11] for $A+A\rightarrow A$ and with earlier $A+A\rightarrow 0$ simulations.[10,12,21] Obviously, the two-dimensional Hertz function is also consistent with $x=1$ (see the Appendix). On the other hand, the critical percolation cluster exhibits $x=1.2$ and the kinetic NNDD's in two dimensions (square lattice) give $x=1.3-1.4$. The latter is consistent with a conjecture[33] discussed below.

IV. DISCUSSION

A. Self-ordering

In all the systems simulated, the ensemble develops from a random particle distribution (Hertz) to a kinetically ordered particle ensemble (KOPE). This transformation is mostly complete in a very short time (order of 100 steps for the densities we studied) and practically steady thereafter. The asymptotic KOPE distribution, which is achieved so rapidly, is obviously a partially *ordered* distribution. Our simulations show the self-ordering pattern for one-dimensional systems (Figs. 1 and 2), two-dimensional (square lattice) systems (Fig. 4), and two-dimensional fractal (percolation cluster) systems (Fig. 5). The self-ordering in the one-dimensional lattice fusion reaction ($A+A\rightarrow A$) follows that predicted by Doering and ben-Avraham[11] for the one-dimensional continuum space (Figs. 2 and 3). For the one-dimensional annihilation reaction ($A+A\rightarrow 0$) the interparticle distribution is consistent (Fig. 3) with the Bramson and Griffeath[23] prediction (for asymptotically large interparticle gaps). This self-ordering underlies the fast change with time of the chemical kinetics formalism[25,29] (see below).

B. Rate laws

The above discussed self-ordering has a drastic effect on the macroscopic kinetic equations.[10] Only a random ensemble is guaranteed to lead to the classical kinetic equation (rate law)

$$-\rho^{-1}d\rho/dt=k\rho\ . \tag{6}$$

Our *ad hoc* assumption replaces[10,25,33] the above equation with

$$-\rho^{-1}d\rho/dt=kP(r\rightarrow 1) \tag{7}$$

for a lattice (with lattice distance normalized to 1). For the $A+A\rightarrow A$ equation in one dimension we obtain from Eq. (1), for the random (Hertz) distribution, $P(r\rightarrow 1)\sim\rho$, in accordance with classical kinetics, i.e., $|d\rho/dt|\sim\rho^2$. However, for longer times, Eq. (2) [with Eq. (7)] gives $P(r\rightarrow 1)\sim\rho^2$. This is in accordance with the third-order rate law ($|d\rho/dt|\sim\rho^3$) discovered in recent years.[22,34] Obviously, there are other possible $P(r)$ distributions that will give the same third-order rate law, such as that of Eq. (5). We note that Eq. (5) is only a crude approximation for the $A+A\rightarrow 0$ reaction, though we know that $|d\rho/dt|\sim\rho^3$ is the correct asymptotic ($t\rightarrow\infty$) rate law.

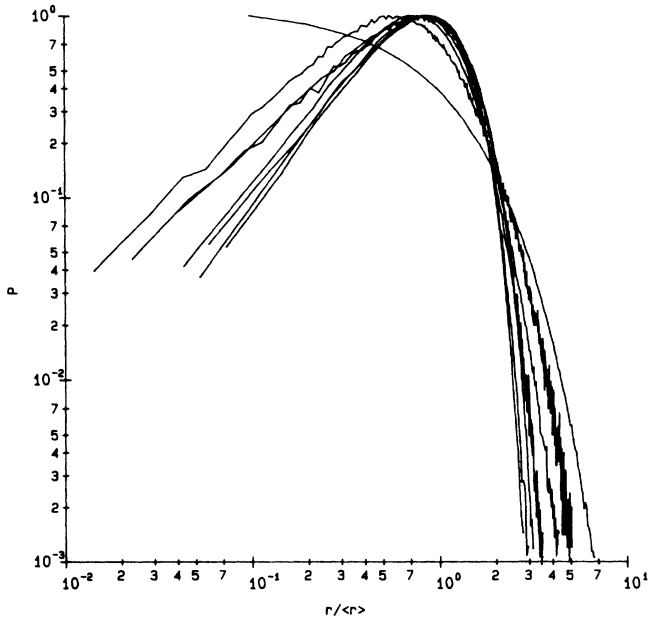

FIG. 6. $P(r)$ vs $r/\langle r\rangle$ in log-log form. Top to bottom (left-hand side): (1) $t=0$, random one-dimensional NNDD; (2) $A+A\rightarrow 0$, one-dimensional NNDD; (3) $A+A\rightarrow A$, one-dimensional NNDD; (4) $t=0$, random two-dimensional NNDD (smoother curve); (5) $A+A\rightarrow 0$, two-dimensional critical percolation cluster NNDD; (6) $A+A\rightarrow A$, two-dimensional critical percolation cluster NNDD; (7) $A+A\rightarrow 0$, two-dimensional NNDD; (8) $A+A\rightarrow A$, two-dimensional NNDD. All curves are for $t=1000$, except the percolation cluster ($t=500$). The data are the same as in the previous figures.

It has been shown that

$$-\rho^{-1}d\rho/dt = k\rho^{1/f}, \quad t \to \infty \tag{8}$$

where f is the time exponent[35,36] in the relation $S \sim t^f$ and S is the number of distinct sites visited by a random walker.[35,36] We can thus hypothesize[33] that, to satisfy Eq. (7), one may have ($t \to \infty$)

$$P(r \to 1) \sim \rho^{1/f} r^{d/f-1} . \tag{9}$$

For $d=1$ ($f=\frac{1}{2}$) this agrees with the analytical solution[11] and for $d=3$ ($f=1$) with the random Hertz distribution.[25]

For the square lattice, the situation is more complex because of the logarithmic corrections in the kinetic expression

$$-\rho^{-1}d\rho/dt = k\rho/\ln\rho . \tag{10}$$

This leads to the expression

$$P(r \to 1) \sim \rho/\ln\rho , \tag{11}$$

with an even more complicated r contribution. Alternatively, for simplicity, effective f numbers have been assigned to the square lattice problems.[3,35,36] A typical value is $f=0.87$, leading to

$$P(r \to 1) \sim \rho^{1.15} r^{1.3} . \tag{12}$$

The power of r ($x=1.3$) is consistent with the simulation result (Fig. 6) which gives $x=1.3-1.4$ (see above). In contrast to this apparent success for the two-dimensional lattice, this approach [Eq. (9)] is suspect for fractals, and does not seem to work for the percolation cluster, where we expect $x=1.9/0.67-1=1.8$ and find only $x=1.2$ from the slopes in Fig. 6.

C. Summary

We have found an important degree of kinetic self-ordering for the $A+A$ reactions up to $d=2$ (we show in the following paper II some residual kinetic ordering even for $d=3$). This is consistent with $d=2$ being the upper critical dimension for $A+A$ kinetic anomalies.[13,22] The self-ordering is surprisingly rapid (almost complete after 100 steps). The kinetically ordered particle ensembles are consistent with the predictions based on analytical approaches.[11,23] There appears to be a simple relation between the NNDD, $P(r)$, and the global rate equation $-\rho^{-1}d\rho/dt \sim KP(r \to 1)$. However, the universality of the global rate equations, i.e., fusion and annihilation reactions giving the same exponents, is not preserved in the self-ordering. Here different $P(r)$ functions are found for fusion and annihilation, giving a *many-to-one* correspondence between $P(r)$ and the global rate law.

ACKNOWLEDGMENTS

We would like to thank Joseph Hoshen for helpful discussions and for suggesting the breadth-first search algorithm. This work has been supported by the National Science Foundation Grant No. DMR-8801120 and by the donors of the Petroleum Research Fund, administered by the American Chemical Society.

APPENDIX: HERTZ DISTRIBUTIONS FOR TAXICAB GEOMETRIES

The generalized Hertz distribution for all dimensions (including fractals[33]) is

$$P(r) = A\rho \exp(-\rho V) , \tag{A1}$$

where V is the volume of a sphere of radius r and A its surface area. For a continuum Euclidean space $V=\alpha_i r^i$ and $A=i\alpha_i r^{i-1}$, so that

$$P(r) = in\alpha_i r^{i-1} \exp(-n\alpha_i r^i) . \tag{A2}$$

We note that for a taxicab geometry Eq. (A1) can be used [but not (A2)]. For a square lattice the two-dimensional "sphere volume" is[37]

$$V = (r+1)^2 + r^2 = 2r^2 + 2r + 1 , \tag{A3}$$

and the one-dimensional "sphere area" is

$$A = 4r + 2 , \tag{A4}$$

giving a Hertz function

$$P(r) = (4r+2)\rho \exp[-\rho(2r^2+2r+1)] \tag{A5}$$

which for $r \gg 1$ is approximately equal to

$$P(r) \cong 4\rho r \exp(-2\rho r^2) . \tag{A6}$$

This should be contrasted with the two-dimensional continuum result (from A2)

$$P(r) = 2\pi\rho r \exp(-\pi\rho r^2) . \tag{A7}$$

From our simulations we find that

$$\rho\langle r\rangle^2 \cong \pi/8 . \tag{A8}$$

Combining (A6) with (A8) gives Eq. (3) (text)

$$P(r) = (\pi/2)(r/\langle r\rangle)\exp[-(\pi/4)(r/\langle r\rangle)^2] . \tag{A9}$$

[1] M. V. Smoluchowski, Phys. Z. **17**, 585 (1916).

[2] S. Chandrasekhar, Rev. Mod. Phys. **15**, 1 (1943).

[3] R. Kopelman, in *Unconventional Photoactive Solids,* edited by H. Scher (Plenum, New York, 1988), pp. 11, 21, 29, 63, 83.

[4] P. G. de Gennes, J. Chem. Phys. **76**, 3316 (1982).

[5] D. C. Torney and H. M. McConnell, Proc. R. Soc. London, Ser. A **387**, 147 (1983).

[6] D. C. Torney and H. M. McConnell, J. Phys. Chem. **87**, 1941 (1983).

[7] R. Ziff, in *Kinetics of Aggregation and Gelation,* edited by F. Family and D. P. Landau (North-Holland, Amsterdam, 1988), p. 191.

[8]N. G. van Kampen, *Stochastic Processes in Physics and Chemistry* (North-Holland, Amsterdam, 1981).
[9]G. Zumofen, A. Blumen, and J. Klafter, J. Chem. Phys. **83**, 3198 (1985).
[10]R. Kopelman, Science **241**, 1620 (1988).
[11]C. R. Doering and D. ben-Avraham, Phys. Rev. A **38**, 3035 (1988).
[12]S. J. Parus and R. Kopelman, Phys. Rev. B **39**, 889 (1989).
[13]A. A. Ovchinnikov and Ya. B. Zeldovich, Chem. Phys. **28**, 215 (1978), and references therein.
[14]A. Blumen, J. Klafter, and G. Zumofen, in *Optical Spectroscopy of Glasses,* edited by I. Zschokke (Reidel, Dordrecht, 1986), p. 199.
[15]K. Kang and S. Redner, Phys. Rev. Lett. **52**, 955 (1984).
[16]P. Meakin and H. E. Stanley, J. Phys. A: Gen. Phys. **17**, L172 (1984).
[17]L. W. Anacker and R. Kopelman, Phys. Rev. Lett. **58**, 289 (1987).
[18]D. ben-Avraham and C. R. Doering, Phys. Rev. A **37**, 5007 (1988).
[19]K. Lindenberg, B. J. West, and R. Kopelman, Phys. Rev. Lett. **60**, 1777 (1988).
[20]S. Kanno, Prog. Theor. Phys. **79**, 721 (1988).
[21]R. Kopelman, S. J. Parus, and J. Prasad, Chem. Phys. **128**, 209 (1988).
[22]Z. Racz, Phys. Rev. Lett. **55**, 1707 (1985).
[23]M. Bramson and D. Griffeath, Ann. Probab. **8**, 183 (1980).
[24]P. Hertz, Math. Ann. **67**, 387 (1909).
[25]G. H. Weiss, R. Kopelman, and S. Havlin, Phys. Rev. A **39**, 466 (1989).
[26]E. Horowitz and S. Sahni, *Fundamentals of Computer Algorithms* (Computer Science, Potomac, MD, 1978).
[27]J. Hoshen and R. Kopelman, Phys. Rev. B **14**, 3438 (1976).
[28]P. Argyrakis and R. Kopelman, J. Phys. Chem. **91**, 2699 (1987).
[29]P. Argyrakis and R. Kopelman, J. Phys. Chem. **93**, 225 (1989).
[30]P. Argyrakis and R. Kopelman, Phys. Rev.. B **31**, 6008 (1985).
[31]E. W. Montroll and W. W. Badger, *Introduction to Quantitative Aspects of Social Phenomena* (Gordon and Breach, New York, 1974), p. 100.
[32]M. Bramson and J. L. Lebowitz, Phys. Rev. Lett. **61**, 2397 (1988).
[33]L. Li, E. Clement, P. Argyrakis, L. A. Harmon, S. J. Parus, and R. Kopelman, in *Fractal Aspects of Materials; Disordered Systems II,* edited by D. A. Weitz, L. M. Sander, and B. B. Mandelbrot (Materials Research Society, Pittsburgh, 1988), p. 211.
[34]L. W. Anacker and R. Kopelman, J. Chem. Phys. **81**, 6402 (1984).
[35]R. Kopelman, J. Stat. Phys. **42**, 185 (1986).
[36]P. Argyrakis and R. Kopelman, Phys. Rev. B **29**, 511 (1984).
[37]J. Hoshen, R. Kopelman, and E. M. Monberg, J. Stat. Phys. **19**, 219 (1978).